J Ther Eng, Vol. 9, No. 4, pp. 901−911, July, 2023

Journal of Thermal Engineering
Web page info: https://jten.yildiz.edu.tr
DOI: 10.18186/thermal.1329554

Journal of Thermal Engineering

Research Article

Measurements of heat transfer coefficients from supercritical fluid flowing in vertical mini channels with constant wall temperature

Ameer Abed JADDOA[1]

[1]*Department of Electromechanical Engineering, Technology University, Baghdad, 19006, Iraq*

ARTICLE INFO

Article history
Received: 06 October 2021
Revised: 17 November 2021
Accepted: 28 November 2021

Keywords:
Heat Transfer; Pressure Drop; Supercritical Fluid CO_2; Mini Channels

ABSTRACT

Currently, efficient heat transmission for compact electronic elements is an essential matter. It needs a heat sink with a liquid cooling scheme that meets these demands as much as feasible. The dimensions of 50.8 × 40.6 × 5.5 mm were adopted for features of heat transfer as well as the fluid flow of supercritical CO_2 in the heat sink in this study. The adopted pressures, temperatures, and mass velocity ranges were 7.5 to 12 MPa, 35 to 50°C, and 100 to 500 Kg/m^{2}s, respectively, wherein the CO_2 cooled under these conditions. The factors of heat transfer, the pressure at levels of local as well as medium degree were determined under these conditions. The medium temperature of CO_2 in the adjacent significant point area increased, the pressure decreased and the medium temperature movement factor augmented dramatically. It was also noted that the medium temperature movement factor peaked at the pseudo-critical temperature. However, the maximum temperature movement factor declined increased pressure. Furthermore, in contrast to the pressure factor, it was revealed that mass velocity and temperature movement factor had a direct relationship. Using the obtained data, a novel correlation mechanism for limited convection of super-critical CO_2 in regular multi-port micro tubes based on chilling conditions was constructed using the obtained coefficients in this study.

Cite this article as: Jaddoa AA. Measurements of heat transfer coefficients from supercritical fluid flowing in vertical mini channels with constant wall temperature. J Ther Eng 2023;9(4):901−911.

INTRODUCTION

The requirement for liquid cooling in much small electronic equipment and other electrical devices has become a key source of concern in recent years in terms of modernization and technical growth. Electronic circuits generate heat that must be dispersed outside of the appliances, thus different cooling systems are required for these devices to function accurately and efficiently. Heat sink cooling systems deems an interesting subject of research in recent years. In this vein, single-phase forced convection in a heat sink that is highly super-cooled is a powerful chilling method with a wide variety of utilization. Among these applications are magnets high voltage systems, pressurized nuclear fission systems, spacecraft applications such as thermal administration systems, electronic device industrialization [1].A supercritical fluid is kept at just over its

*Corresponding author.
*E-mail address: ameer.a.jaddoa@uotechnology.edu.iq

This paper was recommended for publication in revised form by Regional Editor Yaşar İslamoğlu

stringent level of temperature and pressure known as a critical point. Over (304.25 K) and (72.9 atm or 7.39 MPa) for temperature and pressure, respectively, at the critical level, CO_2 acts as a supercritical liquid, expanding to fill its vessel like a gas in the form of density liquid. Besides that, in the case of heating the fluids up to the 304.25 K and compressed thereafter just over 7.39 MPa, then it transfers to the supercritical phase. Under these conditions, it can dramatically modify its characteristics, for instance, solvent power. In the following paragraphs, an overview of supercritical CO_2 applications was introduced. To obtain supercritical states, supercritical carbon dioxide $SCCO_2$ provides a suitable feature of pressure compound with temperature. For most $SCCO_2$-phobic materials, $SCCO_2$ might not be the best solvent. Yet, both silicon and fluorine-products are CO_2-philic and thus likely further soluble. It is well known that magnetic media are made from such products. These products are applied in the manufacture of magnetic media and it deems belong to the earliest utilisations of $SCCO_2$ investigated. In the literature, experiments were conducted for the following cases: aligned channels, perpendicular channels, perpendicular packed bed channels, perpendicular annulus, tube-in-tube, and perpendicular normal circulation tube forms, micro-porous media along with one more structure by researchers [2-6]. On the other hand, temperature movement was greatly improved in the adjacent region of the critical area, with the greatest temperature movement parameters happening at the analogous pseudo-critical temperature. Such improvement was achieved according to an experimental study of supercritical carbon dioxide flow and heat transfer in multichannel mini ports based on cooling conditions. It is interesting to note that temperature movement of liquid acting beneath or nearby supercritical circumstances for different material properties has received much more attention in the literature [7]. Petukhov [8], Hall [9], and Polyakov [10] introduced extensive assessments. In the near-critical zone, Ghajar [11] examined the available empirical methodologies for constrained convective temperature movement. The author discovered that Dittus-Boelter-type correlations could be used to estimate tumultuous constrained convective temperature movement in the adjacent-critical region, whereas the property ratio technique was suggested to estimate substantial differences in physical characteristics. Thereafter, Pitla et al. [12] created a new correlation based on experimental data and numerical calculations to prophesy the temperature movement of supercritical CO_2. The majority of these recent studies made use of considerable or standard channels. Heat transfer measurements were carried out by Liao and Zhao [13] for supercritical CO_2 influx in flat mini/micro circular channels chilled by a stable temperature liquid. The authors discovered a significant disagreement among their outcomes and results that existed in the prior researches, which they attributed to the buoyancy impact occurring in regular channels of great tubes dimensions. In terms of relevant dimensionless parameters, the researchers provided experimental relationships for the axially averaged Nusselt number [14, 15]. Acosta et al. [16] looked at momentum and mass transport in tight rectangular tubes using diameters of 0.96 and 0.38 mm, respectively, of hydraulic tubes. The authors investigated both laminated flux and turbulence situations. Correlations with greater tubes were stated to be satisfactory, and the heat and mass transfer similarity led to the conclusion that heat transfer correlations should be acceptable as well. However, it was discovered that the walls made of optical materials were required to meet the hydraulic smoothness status. Furthermore, the surface roughness had a significant impact on both the friction coefficient and the mass movement factor. For mini/microtubes or channels with cooling conditions, the convection heat transfer of fluids at supercritical pressures was also explored. An investigation was conducted by Pettersen [17] to examine the average heat transfer factor of supercritical CO_2 in multi-port mini-channels based on an inner diameter of 0.79 mm for chilling conditions. The author discovered that Gnielinski's relationship for the one-phase temperature movement factor corresponds to experiment data adequately. In regular mini/micro rotational pipes of 0.50, 0.70, 1.1, 1.40, 1.55, and 2.16 mm diameter chilled to a stable temperature, Liao and Zhao [18] studied axially-averaged convection temperature movement to supercritical CO_2. In this vein, the researchers discovered that the buoyancy impact for constrained heat transfer of supercritical CO_2 over regular pipes at maximum Reynolds numbers was still significant, and they improved the relationship for the axially-averaged Nusselt number for constrained heat transfer of supercritical CO_2 in regular mini/microtubes. In [19-23], the researchers studied the influence of mass influx, pressure, and temperature influx on the axially-averaged temperature movement factor and pressure reduction of carbon dioxide at critical compressing based on chilling circumstances for regular chilling pipes with dimensions changing from 1 to 6 mm of diameters, and suggest a new Gnielinski formula by suitably choosing the standard heat level. It was noted that the majority of current work on supercritical CO_2 concentrated on averaged properties, with a relatively little study on local temperature movement and compression loss, especially for narrow pipes. Many relationships, notably Dittus-Boelter kind or Nu = C Rem Prn, were created and utilized for constrained heat transfer prediction, and the property proportion and standard heat approach were used to integrate varying-properties impacts. However, because the events are so complex, it is widely accepted that the relations do not demonstrate enough concurrence with trials and should only be employed in certain circumstances.

This paper describes an experimental examination of supercritical CO_2 heat transfer and flow features in minor tubes under chilling for a couple of local and averaged through the entire region of the test. A comparison was conducted among the results available in the literature with the experimental results. Consequently, an empirical

correlation was developed. The impacts of various factors on heat transfer and pressure drop behaviour were also investigated.

EXPERIMENTAL SET-UP

Photographically and schematically, Figures (1) and (2) depict the experimental rig, respectively. This study used an experimental setup with integrated measurement devices to investigate the temperature movement behaviour of carbon dioxide in a minor heat sink with forwarding fluid flow. The many challenges related to the high-pressure trials need a considerable interval of about 365 days to settle during the test rig's commissioning. Initial exams for system parameters standardisation and fault expectation removed leakage and fluctuation operating issues. Every single running process, the test data collection technique was meticulously replicated. The entrance and outlet heat, the entrance pressure, the pressure decline over the experiment parts, the inflow velocity, the voltages across the heater, the current, and the values of impedance were all measured throughout the experiments. Also, fifteen copper-constantan thermocouples were used to measure the temperature of the nearby tube. The thermocouples were welded to the heat sink's outside surface. The thermocouples were put into mini-channels (0.2 mm deep by 0.2 mm wide) cut into the test section surface throughout the tube. Pre and post the test area, mixers were installed to mix the fluid prior to accurate thermal resistors which were used to measure the inlet and output fluid temperatures. The thermocouples and thermal resistors were gauged, utilizing a steady temperature oil bath, prior to installation. The temperature readings were accurate to within 0.1 degrees Celsius. The entrance pressure was computed with a precision of 0.075 percent of the entire interval of 12 MPa using a pressure gauge transducer (Model EJA430A). A differential pressure transducer (ModelEJA110A) with a precision of 0.075 percent of the whole range of 500 KPa was used to measure the pressure decrease in the test section. A Coriolis-type mass flow metre (Model MASS2100/MASS6000, MASSFLO, Danfoss) was used to measure the mass flow rate. The mass flow meter's nominal range was 0–65 kg/h, with a 0.1 percent accuracy. A vacuum pump was used to empty the test loop before the trials. The test loop was then cleaned three to four times with powerful clear carbon dioxide (99.995 percent). Repeatedly, the pipe was emptied and scrubbed with carbon dioxide. From the compressed CO_2 container, high-pressure carbon dioxide with a clearly of 99.995 percent was delivered into the system at constant pressure with five MPa. The system pressure was raised to the appropriate super-critical pressure using a pressure at maximum level with carbon dioxide pump. The high-pressure carbon dioxide pump was then switched off, and the sluice connecting the system under investigation to the high-pressure carbon dioxide pump was shut down. The super-critical magnetic pump circulated CO_2 at super-critical pressure. Several experiments revealed that even at considerable pressures, the leakage was relatively modest (e.g. 10 MPa). Silicate glass fibre and sponges were used to insulate the system under investigation and the majority of the loop's system. The mass flow rate, input power, and inlet fluid temperature were all kept constant for each

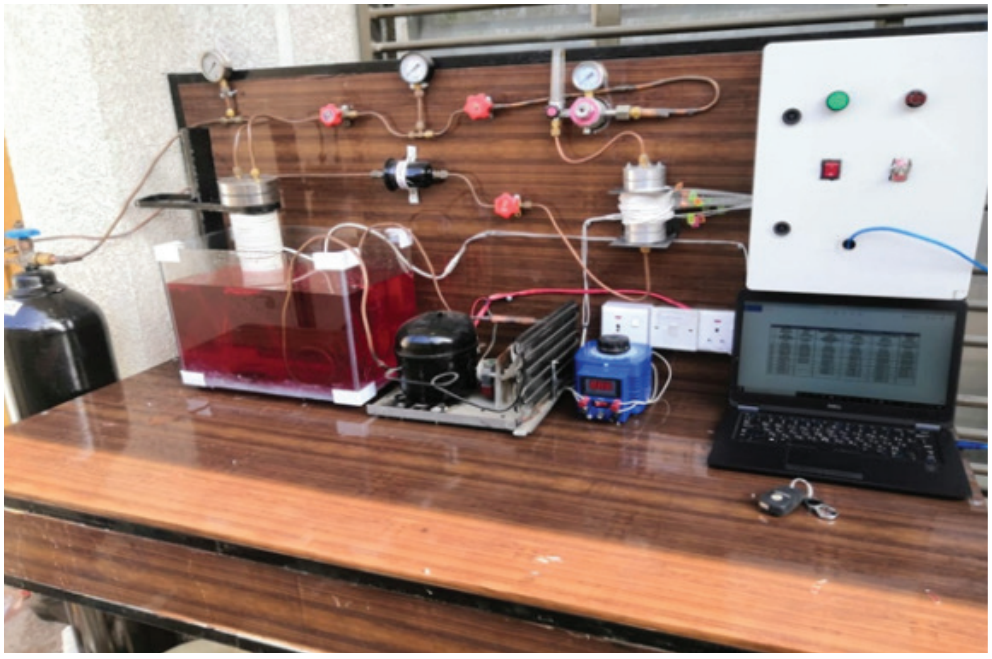

Figure 1. Supercritical carbon dioxide experiment set-up (Photo).

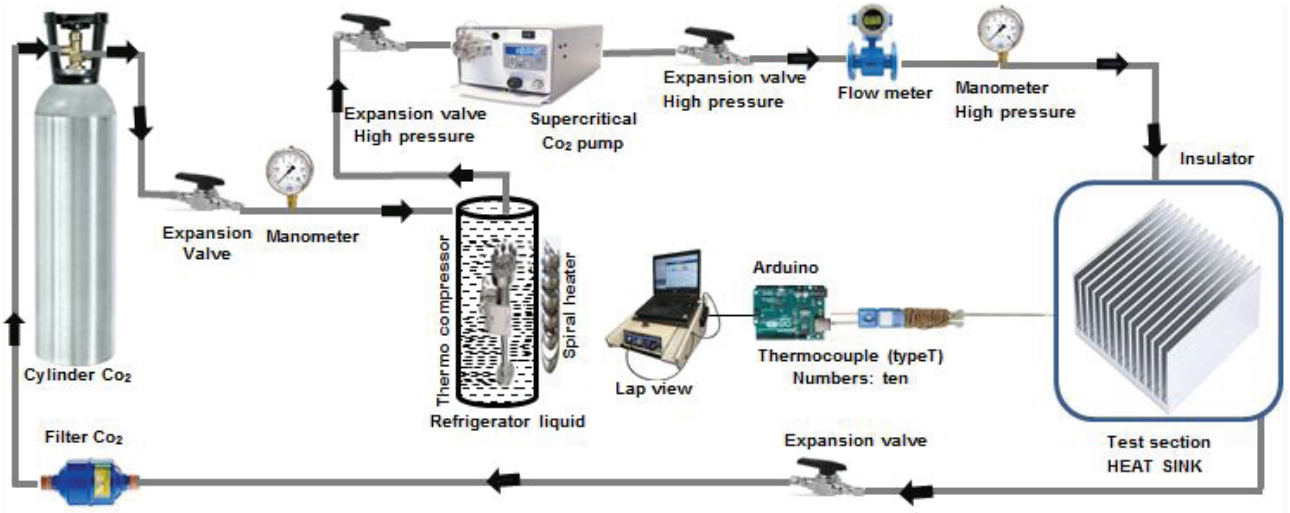

Figure 2. Schematic of a test rig in action.

test. A data extract device (HP 34970A) and an individual computer were used to connect all the measuring instruments. Post the steady-state conditions were established, heat, mass inflow rate, intake pressure, and pressure decline were observed and documented. In addition, the current-voltage values over the heater were measured. The input and output heat, as well as the inflow rate and input voltage, were used to determine the local bulk medium liquid heat at each testing step. The rise in fluid enthalpy was compared to the electric power input. The heat balancing experiment had a 5% experimental uncertainty. In the studies, the system took a long time to attain a steady-state (50–120 minutes). Temperature, input pressure, and inflow rate fluctuations were continually documented throughout the initial transients. During at least 10 minutes, the system was determined to be in a steady state when the changes of the wall temperatures, inlet and outlet fluid temperatures, and inflow rate and input pressure were set about 0.1C. In addition, the flow rate and inlet pressure were all within 0.2 percent. Experimental error in the temperature stability, axial thermal conduction in the system under investigation, erroneous calculated temperature, and the calculation of the temperature movement surface were the main causes of test doubt in the convection heat transfer coefficients. For the small heat sink, the root-mean-square experimental doubt of the convective temperature movement factor was expected to be 11.3 percent. The inlet pressure experimental errors were calculated to be 0.09 percent.

Test section (heat sink)

The heat sink in Figure 3(a) was made of copper 360 alloys with dimensions of 50.8 mm x 40.6 mm and a thickness of 5.5 mm. A heat sink is made up of 17 fins and 16 channels, each with a rectangular cross-section and a hydraulic diameter of 1.5 mm. Figure 3(b) depicts the

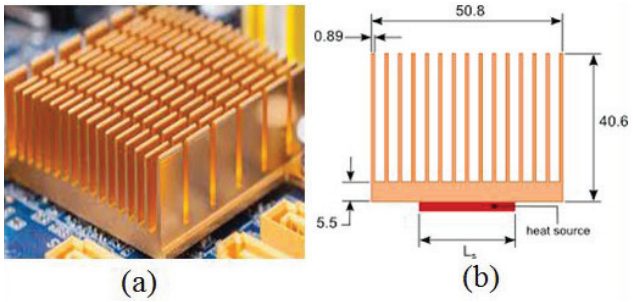

Figure 3. (a) Configuration of heat sink, (b) Heat flux cooling application.

channel width, height, and thickness, as well as all other measurements.

When the mini heat sink was heated instantly with a low voltage A.C current, the temperature transfer in the pipe can be presumed to be single dimension material with an implicit heat generation. The outer surface was isolated, and thermocouples were used to measure the mini heat sink surface temperatures, T_{wo} (x). T_{wi} (x), the surface's regional temperatures, were computed as:

$$T_{wi} = T_{wo} + \left[\left(\frac{q}{16k}\right)(l_o - w_i)^2\right] + \ln\left(\frac{l_o}{w_i}\right)\left[\left(\frac{q}{8k}d_i^2\right)\right] \quad (1)$$

The pipes were winded by the cable to heat the small heat sink. Utilizing the calculated heat value, T_w (x), of the plat, temperatures of the temperature movement surface were estimated.

$$T_{wi}(x) = T_{w\psi}(x) - \ln\frac{l+2\psi}{l}\frac{qw}{2ks} \quad (2)$$

At each axial point, the domestic temperature movement factor, h_x, and the Nusselt value, N_{ux}, were determined as follows:

$$h_x = \frac{q}{(T_{wi} - T_f)}(x)\,, Nu_x = \frac{h \times l}{K_{f,b}}(x) \quad (3)$$

Using the local bulk liquid formation enthalpy, $h_{f,b}$ (x), the domestic bulk liquid heat, Tf,b (x), was estimated.

$$h_{f,b} = h_{f,o} + \frac{\pi q_x l x}{\dot{m}} \quad (4)$$

In the small heat sink, the mean temperature movement factor, h, and the mean Nusselt value, Num, were computed as

$$h = \frac{q}{T_{wi} - T_f}\,, Nu = \frac{hl}{K_f} \quad (5)$$

The average of entire the domestic wall heat was used to calculate the mean temperature of the heat transfer surface.

$$T_m = \sum_{i=1}^{n} (T_{wi}\Delta x)/L \quad (6)$$

The average of the measured and output liquid heat was used to get the mean liquid temperature, $T_{f,m}$. The Reynolds number is calculated as follows:

$$Re = \frac{4\dot{m}}{l\mu\pi} \quad (7)$$

RESULT AND DISCUSSION

By regularly altering the pressure, heat flux of the surface, the interior temperature, and the CO_2 mass quickness, a sequence of experiments were carried out. Figure 4 shows the pressure drop from the test section's intake to exit vs CO_2 average temperature at a particular pressure of 9.0 MPa beside different accelerations ranging from 100 to 500 kg $m^{-2}s^{-1}$, respectively. It's worth noting that the pressure reduction in Figure 4 was measured in kPa, which is substantially lower compared with the total working pressure of the tests, which is 8.0 MPa. Additionally, in the case of the average temperature of carbon dioxide is lower/greater than the pseudo-critical heat, the pressure reduction augmented progressively with augmenting the average temperature of carbon dioxide. In the same context, when the average heat of CO_2 is near the pseudo-critical temperature, the pressure reduction increases dramatically owing to the extreme change in its material characteristics. It might be conclusively proven that the mass acceleration has a meaningful impact on pressure reduction. In a brief statement, the greater the pressure reduction, the greater the mass velocity.

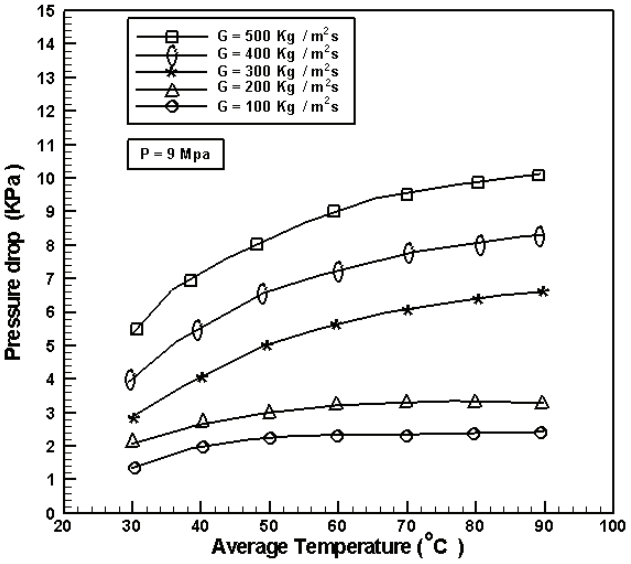

Figure 4. CO_2 average temperature vs. pressure decrease at various mass velocities.

Figure 5 displays the performance for various running pressures (ranging from 7.5 to 12 MPa) and mass velocities (ranging from 100 to 600 kg/m^2 s). Through this study, it can clearly be seen that during the interval of the average heat of carbon dioxide was lower or equal to the pseudo-critical heat (T_{pc}= 32°C at P = 7.5 MPa and T_{pc}= 36°C at P= 12MPa), see Figure 6, the pressure decline continuously augmented as the average heat of carbon dioxide was increased. Owing to the substantial difference in CO_2's physical properties, the pressure decline augmented drastically as the average heat increased near the pseudo-critical point. The mass

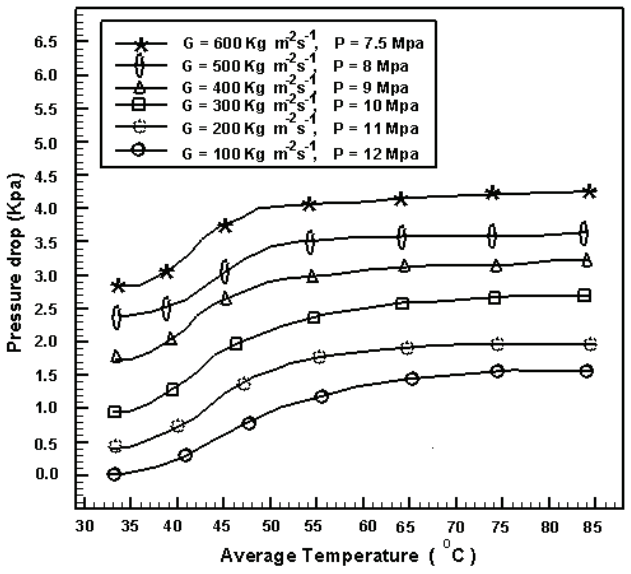

Figure 5. CO_2 average temperature vs. pressure drop for various mass velocities and pressures.

velocity, as expected, has a major impact on the pressure drop. In addition, at a constant operating pressure, the pressure reduction increases with mass velocity; that is to say the bigger the pressure drop, the higher the mass acceleration. in this respect, because the difference in physical characteristics grows smaller as the running pressure increases, the pressure drop reduces for a fixed mass velocity.

For system parameters P= 9 MPa, G= 288 kg m^2s^{-1}, and T_{in}= 33°C, Figure 6 shows standard alteration in the domestic pressure P, the pseudo-critical heat T_{pc}, the domestic bulk mean heat of carbon dioxide T_{bm}, and the domestic interior wall heat T_{wi} over the experiment system under investigation, besides the calculated input and output heat of carbon dioxide T_{bm}. Because the pressure decrease over the experiment segment is so modest, the related pseudo-critical heat remains nearly constant. In the current cooling condition, the heat value was dropped over the inflow direction of carbon dioxide. The estimated carbon dioxide temperatures at the input and outflow were matched the test data quite well.

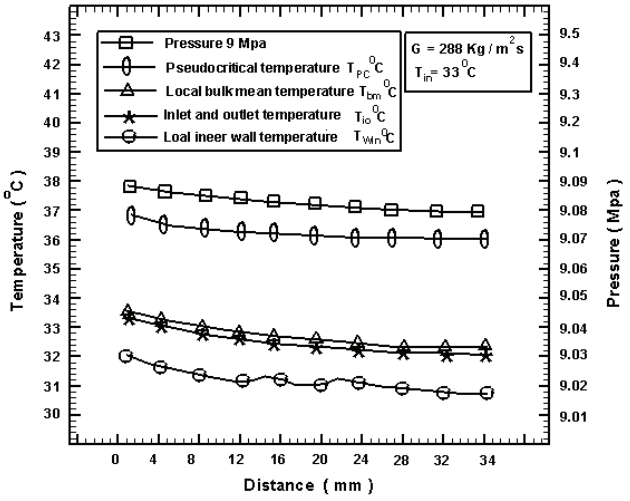

Figure 6. Performance of pressure and temperature against distance.

Along the test segment, Figure 7 depicts the related fluctuations in the local temperature influx and the local temperature movement factor. Both the inner wall temperature and the temperature movement factor show some oscillations. A consequence of this is that owing to a lack of ideal correlation between the cooled copper blocks and the exam sample through the testing. However, the measured parameters remain indicates evidence of the general tendency of fluctuation in the temperature flow and temperature movement factor: the temperature influx and temperature movement factor dropped as the temperature of CO_2 approaches the pseudo-critical temperature along the test segment.

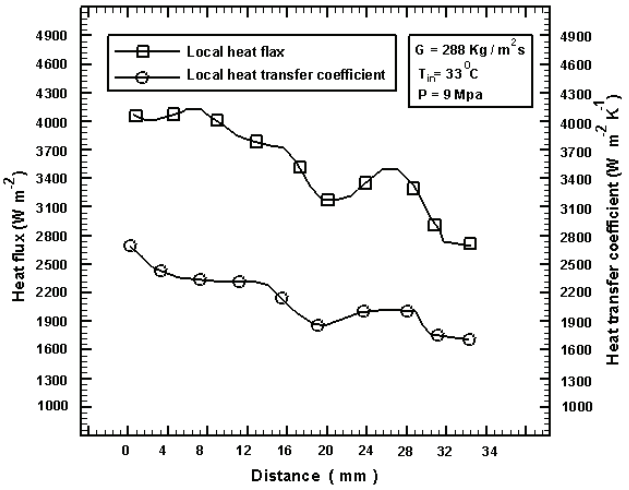

Figure 7. Performance of heat influx and temperature movement factor against distance.

At varying inlet temperatures of CO_2 Tin from 35 to 50°C, Figures 8 and 9 show the fluctuation of domestic pseudo-critical heat T_{pc}, domestic bulk average heat of carbon dioxide T_{bm}, and domestic temperature factor α over exam segment. The relevant working conditions were adopted in this work as P= 9.5 MPa and G= 210 kg m^{-2} s^{-1}. The situation with T_{in}= 48°C, which is the nearest to the pseudo-critical heat of carbon dioxide, 39°C, yields the highest temperature movement factor, as seen in Figures 8 and 9. Considering the particular temperature achieves a maximum magnitude at the pseudo-critical level, a maximum temperature movement factor is obtained as the heat of carbon dioxide is near to the pseudo-critical heat. This finding shows that CO_2 temperature has a considerable impact on temperature movement around the pivotal point and that the maximum temperature movement average appears in this zone.

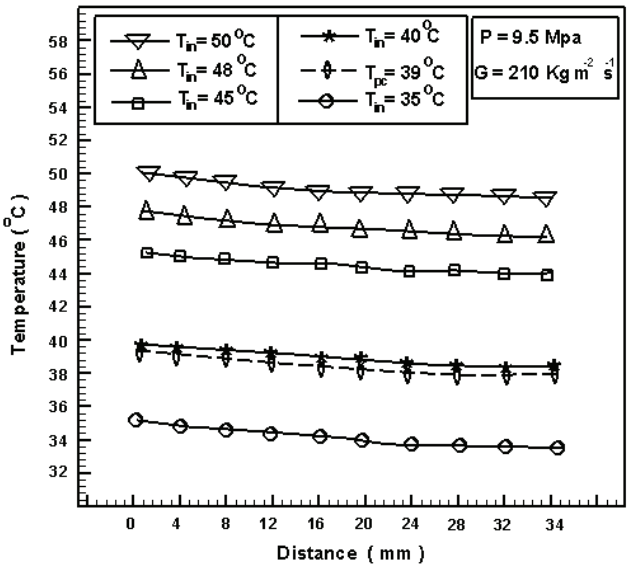

Figure 8. Local temperature fluctuations along the test segment.

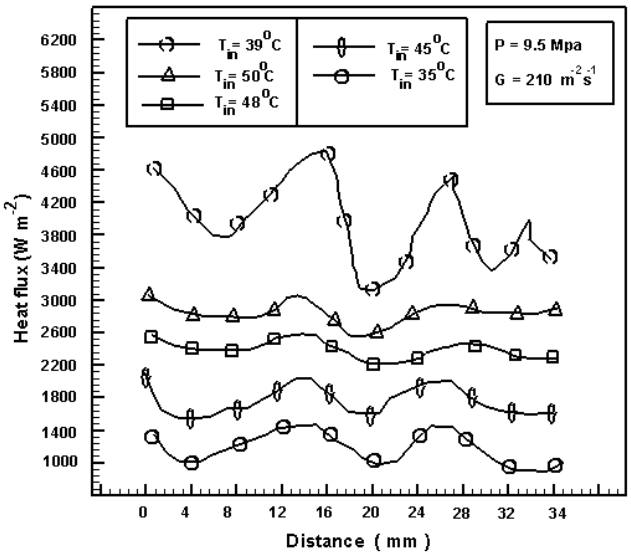

Figure 9. Differences in domestic temperature movement factor accompanying the rig-test segment.

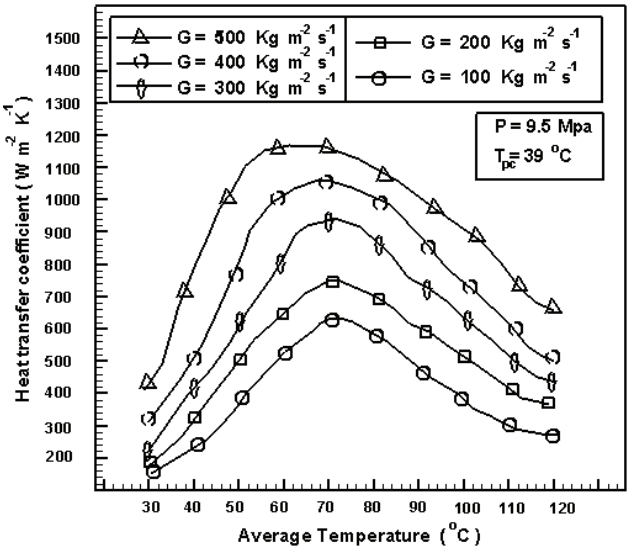

Figure 11. CO_2 average temperature vs. heat transfer coefficient average.

The significant shift of material characteristics for instance density, specified temperature, viscosity, and electric accessibility is amongst the most essential aspects of supercritical liquids in the close-critical zone. Figure 10 depicts typical CO_2 specific heat fluctuations in terms of heat based on different pressures (7.5, 8.0,10,11 and 12 MPa). At the close of the pseudo-critical heat zone, which matches the maxim of specified temperature at the working pressure, a drastic change may easily be seen. CO_2's temperature movement and inflow properties may vary significantly compared to steady characteristic liquids as a result of these changes in fluid property.

Figure 11 shows how the rate temperature movement factor varies with CO_2 temperature rate for a specific system pressure of P= 9.5 MPa and mass velocities ranging from G= 100 to 500 kg $m^{-2}s^{-1}$. At each mass velocity, the rate of temperature movement factor augmenters rapidly in the close-critical zone, peaking around the identical pseudo-critical heat (T_{pc}= 39°C at P = 9.5 MPa). As illustrated in Figure 10, the exceptionally increase of temperature movement rate nearby the pseudo-critical heat zone is because specific heat varies similarly throughout the region near the critical point. Furthermore, the higher temperature movement factor grows individually with mass acceleration for the given operating pressure of 9.5 MPa, implying that mass acceleration has a considerable impact on temperature movement performance.

Figure 12 illustrates the impact of the adopted system pressure on the temperature movement factor rate; the adopted parameters of this work were pressure 7.5 - 12

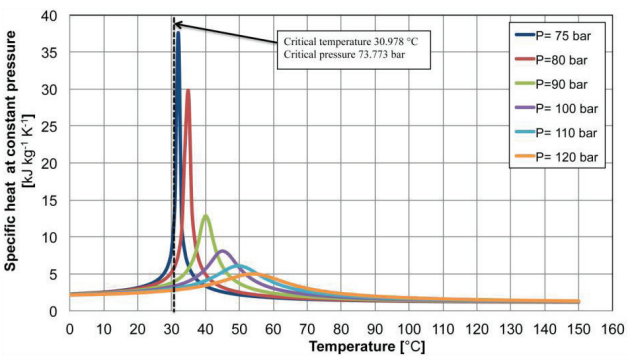

Figure 10. Variation of specific heat of CO_2 at P = 7.5, 8.0, 9, 10, 11, and 12 MPa.

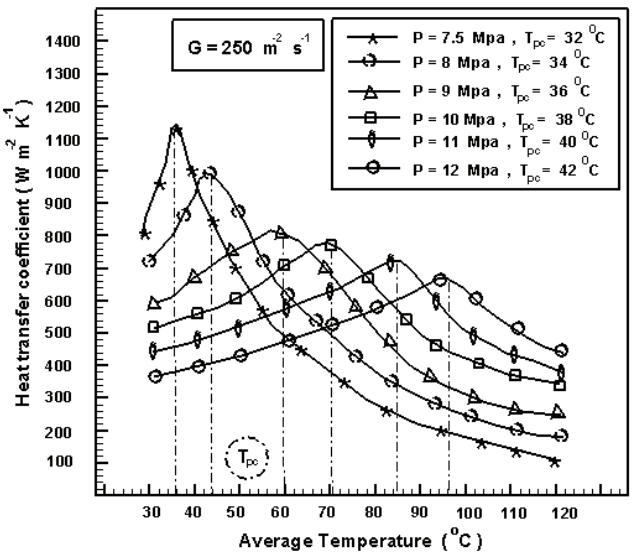

Figure 12. Differences of CO_2 average temperature vs. heat transfer factor average.

MPa, and mass velocities 250 kg/m^{2}s. Figure 12 demonstrates a comparable difference in the temperature movement rate in degree with the heat rate of carbon dioxide presented in Figure 11. That is to say, a direct relationship between increasing the CO_2 temperature and the average heat transfer degree. Wherein, it is to reach the maximum level rapidly at the adopted pseudo-critical heat. T_{pc}= 32°C at Pressure 7.5 MPa, Pseddocritical temperature 34°C at Pressure= 8.0 MPa, Pseddocritical temperature 36°C at Pressure 9 MPa, Pseddocritical temperature 38°C at Pressure 10 MPa, Pseddocritical temperature 40°C at Pressure 11 MPa, Pseddocritical temperature 42°C at Pressure 12 MPa. According to the same specific heat difference at the precise pressure in which the obtained results in Figure 10 was achieved, the maximum level of heat transfer average factor increases as the pressure decreases at 10-12 MPa.

Dimensional numbers, many relationships between the Nu and Re and other suggested in the literature. The results of the current experiment are compared to the 5 most significant correlations suggested by [Huai-Koyama, Di-Boelter, Gnielinski, Pe-Popov, Pitla, and Li-Zhao]. Figures 13 and 14 shows a comparison predicted by 5 correlations in the literature for local Nusselt number along the test section a with experimental data; Figure 13 for the case of pressure 8 MPa, mass velocities= 350 kg/ m^{2}s, and temperature inlet 31°C, and Figure 14 for the case of Pressure 8 MPa, mass velocities 350 kg/ m^{2}s, and temperature inlet 55°C, respectively. A comparison of the cases experimentally investigated for local Nu over the test segment with those estimated in the literature for 5 relationships. All correlations have indicated a smooth change in the local Nu, but the present experimental data show some fluctuation in the local Nu along the test section. The Pe-Popov correlation, in particular, is much overestimated; since the relationship was formed using data from larger diameter tubes and is therefore unsuitable for the current small diameter tubes. Hu– Koyama, Di-Boelter, Gnielinski, and Pitlas other three correlations all indicate a proper order of magnitude for the local Nu.

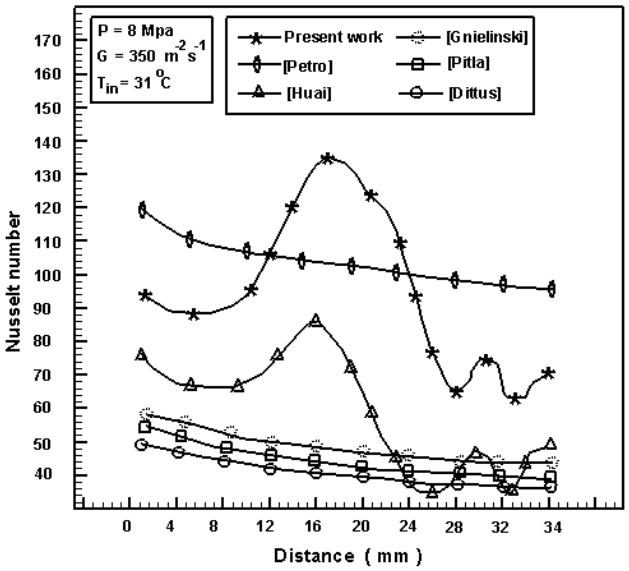

Figure 13. Comparison of experimental data with for the case of Pressure 8 MPa, mass velocities 350 kg/m^{2}s and Temperature inlet = 31°C.

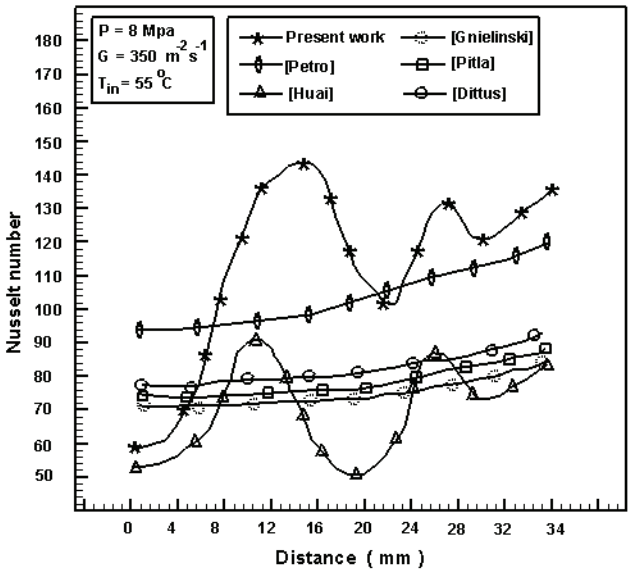

Figure 14. Experimental data comparison for the case of pressure 8 MPa, mass velocities 350 kg/m^{2}s, and temperature inlet 55°C.

All correlations have indicated a smooth change in the local Nusselt number, but the current experimental data show some fluctuation in the local Nusselt number along the test section. The Petrov-Popov correlation, in particular, is much overestimated; since the relationship was formed using data from larger diameter tubes and is therefore unsuitable for the current small diameter tubes. Huai – Koyama, Dittus-Boelter, Gnielinski, and Pitla's other three correlations all indicate a proper order of magnitude for the local Nusselt number. The average Nusselt numbers achieved in this study in terms of CO_2 average temperature are compared to estimation utilizing Dittus-Boelter, Gnielinski, and Liao-hypothesized Zhao's correlations. Figure 15 shows the results under the conditions of P= 8.0 MPa and G= 310 kg m^{-2}s^{-1}. It can be demonstrated that all three correlations estimated the highest Nusselt number close to the relevant pseudocritical temperature (T_{pc}= 35°C at P= 8 MPa) and also provide the local Nusselt number with a right order of magnitude

The next experimental relation for constrained convection temperature movement of supercritical carbon dioxide in a regular small heat sink was achieved under a large quantity of experimental data.

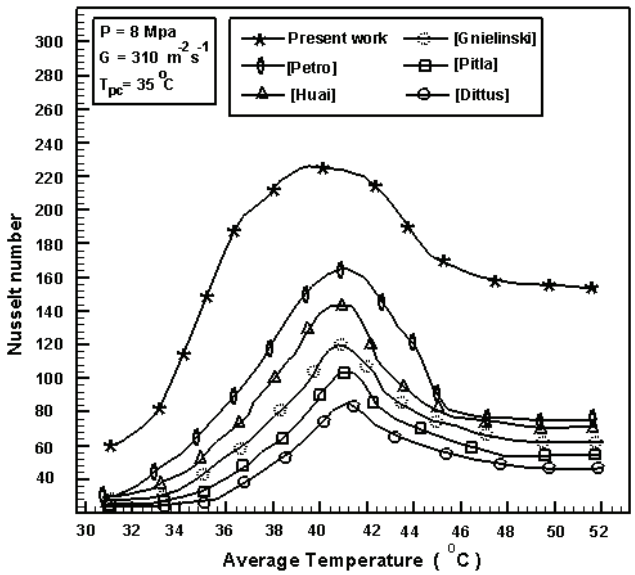

Figure 15. Correlations in the literature with the measured Nusselt number.

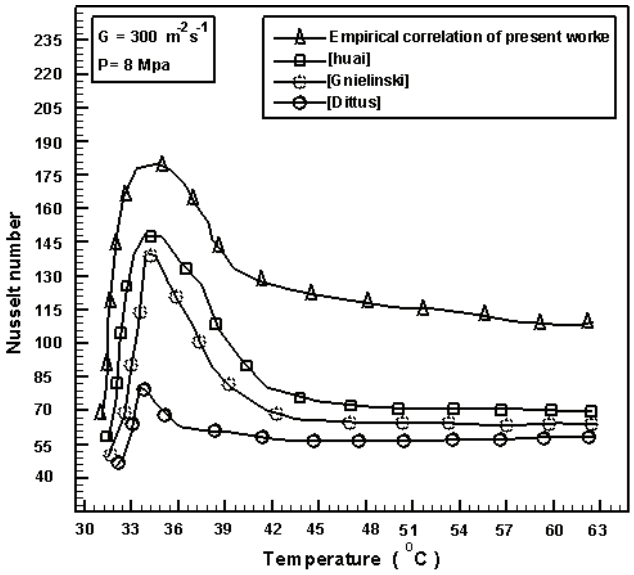

Figure 17. Equation (8) is compared to correlations found in the literature.

$$Nu = 3.34 \times 10^{-1.965} Pr^{0.4} Re^{0.9} \left(\frac{average\ C_\rho}{C_{\rho w}}\right)^{0.099} \left(\frac{\rho_r}{\rho_w}\right)^{-2.23} \quad (8)$$

Where

C_{pw} and ρ_w represents the expected according to wall temperature.

ρr is denotes CO_2 bulk temperature expected value.

Average Cp is determined as $\frac{h_f - h_w}{T_r - T_w}$

The bulk average heat of carbon dioxide is used to determine all physical parameters in Nu, Re, and Pr.

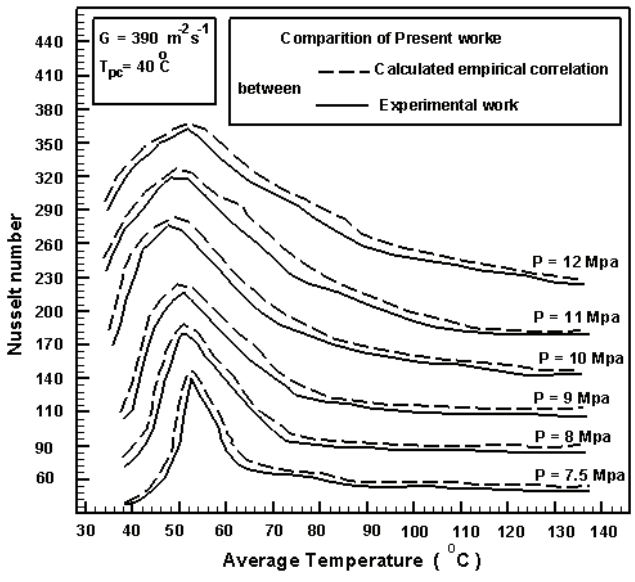

Figure 16. Equation (8) and the experimental Nusselt number are compared.

Equation 8 ranges of application are 7 MPa ≤ P ≤ 12 MPa, 20°C ≤ Tbm ≤ 53°C, 100 kg $m^{-2}s^{-1}$ ≤ G ≤ 600 kg $m^{-1}s^{-1}$, and 1 kW m^{-2} ≤ q ≤ 25 kW m^{-2} . In this scenario as illustrates in Figure 12 (P 7.5, 8.0, and 8.5 MPa, G 209.3 kg m^2s^1), Figure 16 illustrates a comparison of the measured Nusselt value with those computed utilizing the correlation, Equation 8. Clearly, the novel correlation accurately predicts the experimental findings

The obtained results by Equation 8 based on Nusselt value were compared with calculated using Dittus-Boelter and Gnielinski correlations. See Figure 17. In this regard, the comparable adopted limitations of this research were P 8.0 MPa and G= 300 kg $m^{-2}s^{-1}$. The Nusselt number was predicted by three correlations to be in the appropriate order of magnitude, with a maximum variation of roughly 18 percent.

CONCLUSIONS

1. Heat transfer performance is influenced by test section pressure, mass acceleration, and CO_2 heat, notably in the close-critical zone. Meanwhile, as the test section pressure rises, the maximum heat transfer coefficient drops. Also, It was noted that the heat transfer coefficient increases as the mass velocity increases.
2. According to the experimental results, the pressure reduction increases considerably as the average temperature of carbon dioxide in the zone close the pseudo-critical heat increased.
3. The pressure declined was significantly affected by mass acceleration and adopted pressure. Even more, for a fixed operating pressure, the pressure reduction augmented with mass acceleration, however, for a specific

mass acceleration, the pressure reduction declined with adopted pressure. Furthermore, the results of the experiments also showed that CO_2 temperature, operating pressure, and mass velocity all play a vital role in the overall system performance.

4. At nearby-critical zone, temperature movement is substantially improved, at the matching pseudo-critical heat, with the greatest temperature movement factor.
5. For constrained convective temperature movement of supercritical CO_2 in regular heat sink in the chilling situation, a Dittus-Boelter correlation category was obtained based on a significant quantity of experimental data besides the novel correlation accurately matched the experimental results.

ACKNOWLEDGMENTS

Gratefully acknowledgments to Middle Technical University, University of Technology, and Ministry of Industry – Al- Faris Company [P.O.Box: 273, Jubail 31951] for their assistance with all experimental and heat transfer examinations for these studies.

AUTHORSHIP CONTRIBUTIONS

Authors equally contributed to this work.

DATA AVAILABILITY STATEMENT

The authors confirm that the data that supports the findings of this study are available within the article. Raw data that support the finding of this study are available from the corresponding author, upon reasonable request.

CONFLICT OF INTEREST

The author declared no potential conflicts of interest with respect to the research, authorship, and/or publication of this article.

ETHICS

There are no ethical issues with the publication of this manuscript.

NOMENCLATURE

Greek symbols

A	Area surface of the test section, m^2
w_f	Width of test section mm
g	acceleration of gravity, m/s^2
h	coefficient of average heat transfer ,W/m^2K
k	thermal conductivity,W/mK
l_f	test section heated length, mm
T_{wi}	Local temperature along the tese section °C
T_{fb}	The local bulk fluid temperature °C
T_{pc}	Pseddocritical temperature °C
p	Pressure of CO_2 Mpa
T_m	Mean temperature °C
G	Mass velocities $kg\ m^{-2}s^{-1}$
Nu_x	Nusselt number $\frac{\rho u x}{\mu}$
u	Velocity flow of CO_2, m/s
Re_b	Reynolds number ud/v
Δp	Pressure drop difference of CO_2 , bar.
v	Kinematic viscosity of CO_2, m^2/s
ρ	Density of CO_2, kg/m^3
μ	dynamic viscosity, kg/m s

Subscripts

w	Wall
in, out	inlet and outlet CO2 of the test section
b	bulk
f	fliuid
x	axis

REFERENCES

[1] Al Tae'y KA, Jaddoa AA, ABD HS. A loop thermosyphon for liquid cooled minichannels heat sink with pulsate surface heat flux. J Therm Eng 2021;7:1030−1038. [CrossRef]

[2] Bilalov TR, Zakharov AA, Jaddoa AA, Gumerov FM, Le Neindre B. Treatment of different types of cotton fabrics by ammonium palmitate in a supercritical CO2 environment. J Supercrit Fluids 2017;130:47−55. [CrossRef]

[3] Jaddoa AA. Convection heat transfer analysis with flow resistance for mini-helically coiled tubes at supercritical pressures experimentally. Int J Heat Technol 2021;39:817−824. [CrossRef]

[4] Jaddoa AA. Convection heat transfer performance for the Scf-Co2 media in mini-tube with fins experimentally. J Eng Sci Technol 2021;16:3407−3420.

[5] Kkihlefa BJ, Jaddoa AA, Reja AH. Experimental investigation of heat transfer features for vertical tube using porous media and Carbon dioxide. J Mech Eng Res Develop 2021;44:188−195.

[6] Huai X, Koyama S. Heat transfer characteristics of supercritical CO2 flow in small-channeled structures. Exp Heat Trans 2007;20:19−33. [CrossRef]

[7] Huaia XL, Koyama S, Zhao TS. An experimental study of flow and heat transfer of supercritical carbon dioxide in multi-port mini channels under cooling conditions. Chem Eng Sci 2005;60:3337−3345. [CrossRef]

[8] Petukhov BS. Heat transfer and friction in turbulent pipe flow with variable physical properties. Adv Heat Transf 1970;6:504−564. [CrossRef]

[9] Hall WB. Heat transfer near the critical point. Adv Heat Transf 1971;7:1−86. [CrossRef]

[10] Polyakov AF. Heat transfer under supercritical pressures. Adv Heat Transf 1991;21:1−53. [CrossRef]

[11] Afshin JG, Asadi A. Improved forced convective heat transfer correlations for liquids in the near-critical region. AIAA J 1985;24:2030−2037. [CrossRef]

[12] Pitla S, Groll S, Eckhard A, Ramadhyani S. New correlation for the heat transfer coefficient during in-tube cooling of turbulent supercritical carbon dioxide. Int J Refrig 2002;25:887−895. [CrossRef]
[13] Liao SM, Zhao TS. Measurements of heat transfer coefficients from supercritical carbon dioxide flowing in horizontal mini/micro channels. J Heat Transf 2002;124:413−419. [CrossRef]
[14] Gnielinski V. New equations for heat and mass transfer in turbulent pipe and channel flow. Int Chem Eng 1976;16:359−367.
[15] Petrov NE, Popov VN. Heat transfer and resistance of carbon dioxide cooled in the supercritical region. Thermal Eng 1985;32:131−134.
[16] Acosta. R, Muller R, Tobias C. Transno_rt u. rocesses in narrow (capillary) channels. AIChE J 1985;31:473−482. [CrossRef]
[17] Pettersen J, Rieberer R, Leister A. Heat transfer and pressure drop characteristics of supercritical carbon dioxide in microchannel tubes under cooling. Proc. 4th IIR-Gustav Lorentzen Conference on Natural Working Fluids in Purdue, Joint Conference of the International Institute of Refrigeration. Section B and E, 2000. p. 99−106.
[18] Liao SM, Zhao TS. Measurements of heat transfer coefficients from supercritical carbon dioxide flowing in horizontal mini/micro channels. J Heat Transf 2002;124:413−420. [CrossRef]
[19] Dang C, Hihara E. In-tube cooling of supercritical carbon dioxide: Part 1. Experimental measurement. Int J refrigeration 2004;27:736−747. [CrossRef]
[20] Küçükakça Meral Z, Parlak N. Experimental research and CFD simulation of cross flow microchannel heat exchanger. J Therm Eng 2021;7:270−283. [CrossRef]
[21] Vinayak Gaikwad, Suhas Mohite, Swapnil Shinde, Mahesh Dherange, Enhancement in thermo-hydraulic performance of microchannel heat sink with secondary flows of leaf venation pattern. J Therm Eng 2020;6:677−696. [CrossRef]
[22] Ozdemir MR, Sözbir OR. A review of single-phase and two-phase pressure drop characteristics and flow boiling instabilities in microchannels. J Therm Eng 2018;4:2451−2463. [CrossRef]
[23] Cebi A, Celen A, Donmez A, Karakoyun Y, Celen P, Cellek MS, et al. A review of flow boiling in mini and microchannels for enhanced geometries. J Therm Eng 2018;4:2037−2074. [CrossRef]